A Twisted Charge Transfer Structure for All-directional Autofocus CMOS Image Sensor

Daiki Shirahige[1,3], Koichi Fukuda[2,3], Hajime Ikeda[1], Yusuke Onuki[1], Ginjiro Toyoguchi[1], Kohei Okamoto[2], Shunichi Wakashima[2], Hiroshi Sekine[1], Shuhei Hayashi[1], Ryo Yoshida[1], Junji Iwata[1], Yasushi Matsuno[1], Katsuhito Sakurai[1], Hiroshi Yuzurihara[1], Takeshi Ichikawa[1],

[1]Device Technology Development Headquarters, Canon Inc., Kanagawa, Japan
[2]Imaging Business Operations, Canon Inc., Tokyo, Japan
[3]Graduate School of Engineering, Tohoku University, Sendai, Japan
TEL: +81-3-3758-2111
email: shirahige.daiki@mail.canon[1], shirahige.daiki.s2@dc.tohoku.ac.jp[2]

Abstract— We propose a CMOS image sensor with twisted photodiode (PD) for all-directional autofocus (AF) to achieve high speed and high precision AF. The newly developed 3D-stacked back side illuminated (BSI) sensor features a twisted PD that enables vertical phase detection, achieving AF for all pixels and in all directions. In this paper, we introduce the structure of the twisted PD, which enables all-directional AF, and describe the results of our investigation on charge transport in this structure.

I. INTRODUCTION

CMOS image sensors are widely used in many different applications, including mobile, digital still camera, automotive, and security, where they are required to have a variety of functions. In particular, autofocus (AF) is one of the most important functions, and various pixel structures have been developed to achieve faster and more accurate AF [1-3]. The conventional method of dividing pixels into left and right halves allows phase detection for subjects with vertical line patterns, but not for subjects with horizontal line patterns. In order to achieve high-speed, high-precision AF for a wide range of subjects, phase detection auto focus (PDAF) pixels have been developed that use a different pixel division approach.

Table 1 shows a comparison of various PDAF pixel structures. We propose a twisted PD structure in which the pixels are rotated by 90 degrees on the front and back sides. Vertical pixels with this twisted structure are arranged in Gb pixels [4]. The back side of the vertical pixel is vertically separated, which enables phase detection of horizontal line patterns. On the other hand, the front side of the vertical pixel is horizontally separated, and it has the same pixel structure as the horizontal pixel. Therefore, the twisted PD enable phase detection in all directions without any difference in characteristics between vertical and horizontal pixels.

II. SENSOR ARCHITECTURE

Fig. 1 shows the charge transfer paths. The pixel is separated into two PDs by a p-n junction for phase difference detection. Each PD is also separated into a front side and a back side by another p-n junction, and a slit is formed in part of the PN junction. The depletion region is designed to extend to the back side through the slit, and the charge generated by photoelectric conversion at the back side moves to the front side along the electrostatic potential gradient.

Fig. 2 shows the results of 3D potential profile simulation. Both the horizontal and vertical pixels show a monotonic potential distribution from the backside to the frontside. In particular, the vertical pixel is designed so that the direction of PD division is rotated by 90 degrees between the front side and back side, and this enables AF for a subject with a horizontal line pattern in the vertical pixel.

Fig. 3 is a top-view SEM image of the pixels. The vertical pixels are placed in Gb pixels of the Bayer pattern, and the horizontal pixels are placed in R, Gr, and B pixels. Fig. 3 shows that the shapes of the shallow trench isolation (STI) and polysilicon on the silicon surface are the same for the horizontal and vertical pixels. When the STI, polysilicon, and metal wiring of the vertical pixels are rotated by 90 degrees, a difference in shape occurs with the horizontal pixels. Twisted PD suppresses the difference in characteristics by making the silicon surfaces of the horizontal and vertical pixels the same structure.

Fig. 4 shows a cross-sectional TEM image of the pixel, and Fig. 5 shows the results of optical simulations at the center and edge of the sensor. In this image sensor, an inner lens, color filter, and micro lens are placed on the silicon surface, and it is designed so that the incident light is efficiently collected by each PD. The optical structure of the pixel was designed using three-dimensional finite-difference time-domain (FDTD) optical simulation, which demonstrates the position of incident light on the pixels at the center and edge of the

sensor. The simulation was performed on the marginal ray angle at F-number 1.8 for the edge pixels of the chip. The incident angle of the light increases at the edge pixels on the chip, and the light enters off the center of the pixel. The optical simulation results for the chip at the edge of the pixel was used as a reference when determining the light incident position in the device simulation described later.

Fig. 6 shows the results of electrostatic potential simulations along the charge transfer path. The twisted PD has a complex three-dimensional charge transfer path, and it is necessary to form an electrostatic potential which allows an appropriate charge transfer. As shown in Fig. 6, the potential gradient is appropriately formed in the four types of PDs along the path through the slit from the back side to the front side.

III. RESULTS AND DISCUSSION

Fig. 7 shows the number of electrons in the photoelectric conversion region at the back side of the pixel over time. It shows a duration for the generated electrons to move from the back side to the front side of the pixel. It was confirmed that the generated charges move to the charge storage region on the front side of the pixel in a very short time of 10 ns for all of the top, bottom, left, and right PDs.

Fig. 8 shows the current density of top PD at each time after charge generation. This simulation result shows the movement of the charges generated by incident light at the edge of the pixel, with reference to the results of the optical simulation. The charge generated in the photoelectric conversion area moves to the storage area via the slit. As shown in Fig. 7, charge transfer to the charge storage region is completed within 10 ns, and the simulation confirms that rapid charge transfer is achieved without crosstalk to adjacent PDs.

Fig. 9 shows the light sensitivity dependence on incident light angle for vertical and horizontal pixels. Figs. 9(a) and (d) are shown in one-dimension, and Figs. 9(b), (c), (e), and (f) in two-dimensions. Signal levels at the top, bottom, left, and right PDs are indicated as S_T, S_B, S_L, and S_R, respectively. Each PD is sensitive to light with specific incident angles, which indicates that PDs are separated effectively. As shown in Fig. 9, the vertical pixel and horizontal pixel have sensitivity angle characteristics for each angle, and phase difference detection for each direction is achieved.

Fig. 10 shows the results of imaging and phase detection using a CMOS image sensor with a twisted PD. In conventional horizontal AF sensors, the accuracy of AF decreases when the subject contains a horizontal line pattern, whereas vertical AF with a twisted PD achieves more accurate focusing.

Table 2 summarizes the comparison of sensor characteristics to the previous studies [1,3,5-8].

IV. CONCLUSION

In CMOS image sensors for imaging applications, AF is one of the most important functions, and it is required to focus more quickly and precisely on a variety of subjects. We verified that high-precision AF can be achieved by all-directional AF with twisted PD. Although the twisted PD has more complex charge transfer structure than the conventional dual PD, by optimizing the electrostatic potential we confirmed that the charges are transported in an extremely short time without crosstalk.

REFERENCES

[1] M. Kobayashi *et al*., "A Low Noise and High Sensitivity Image Sensor with Imaging and Phase-Difference Detection AF in All Pixels," *Int. Image Sensor Workshop (IISW)*, 24-27, 2015.

[2] K. Fukuda, "A Compressed N×N Multi-Pixel Imaging and Cross Phase-Detection AF with N×1RGrB + 1×NGb Hetero Multi-Pixel Image Sensors," *Int. Image Sensor Workshop (IISW)*, 166-169, 2021.

[3] T. Okawa *et. al*., "A 1/2inch 48M all PDAF CMOS image sensor using 0.8 μm Quad Bayer coding 2×2OCL with 1.0 lux minimum AF illuminance level," *IEEE International Electron Devices Meeting (IEDM)*, 16.3.1-16.3.4, 2019.

[4] D. Shirahige *et al*., "Cross Dual-Pixel Twisted-Photodiode Image Sensor for All-Directional Auto Focus," *IEEE International Electron Devices Meeting (IEDM)*, 1-4, 2023.

[5] E. S. Shim *et al*., "All-Directional Dual Pixel Auto Focus Technology in CMOS Image Sensors," *Symposium on VLSI Circuits (VLSI)*, 1-2, 2021.

[6] T. Jung *et al*., "A 1/1.57-inch 50Mpixel CMOS Image Sensor With 1.0μm All-Directional Dual Pixel by 0.5μm-Pitch Full-Depth Deep-Trench Isolation Technology," *IEEE International Solid-State Circuits Conference (ISSCC)*, 102-104, 2022.

[7] H. Kim *et al*., "A 0.64μm 4-Photodiode 1.28μm 50Mpixel CMOS Image Sensor with 0.98e- Temporal Noise and 20Ke- Full-Well Capacity Employing Quarter-Ring Source-Follower," *IEEE International Solid-State Circuits Conference (ISSCC)*, 1-3, 2023.

[8] Y. Sawai *et al*., "A 5.6μm Stacked Voltage Domain Global Shutter Pixel with 70ke- Linear Full Well Capacity and 85dB Single Exposure High Dynamic Range," *Int. Image Sensor Workshop (IISW)*, 324-327, 2021.

Table 1. Comparison between various PDAF

	Conventional PD	Quad PD	Slanted PD	Rotated PD	Twisted PD (This work)
Plan view					
Pixel structure	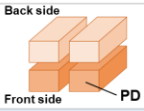	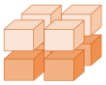		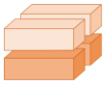	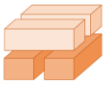
PDAF accuracy	Excellent	Excellent	good	Excellent	Excellent
Vertical PDAF	Poor	Excellent	good	Excellent	Excellent
DRN	Excellent	Poor	Excellent	good	Excellent
FWC	Excellent	Poor	Excellent	good	Excellent
H/V pixel mismatch	Excellent	Excellent	Excellent	Poor	Excellent
Readout time	Excellent	Poor	Excellent	Excellent	Excellent
Data processing	Excellent	Poor	Poor	Excellent	Excellent

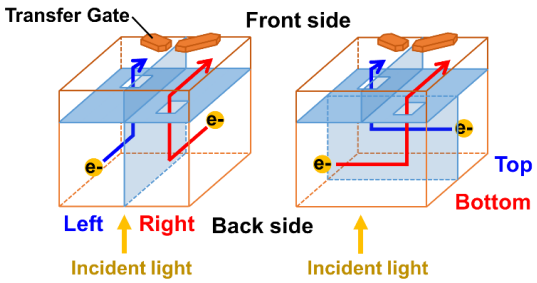

Fig. 1. Charge transfer paths.

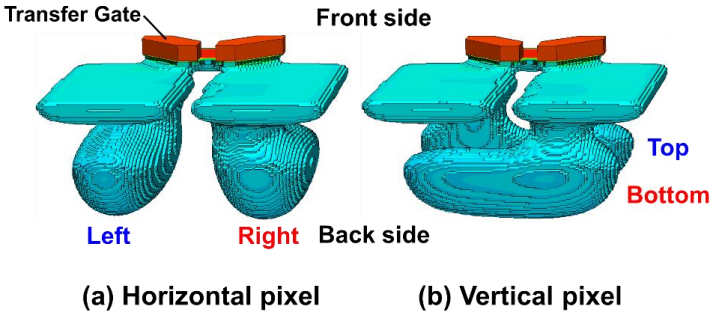

Fig. 2. 3D TCAD simulation results for potential profiles.

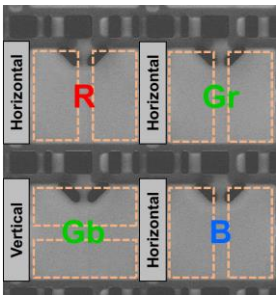

Fig. 3. Top view of scanning electron microscope (SEM) of the pixels.

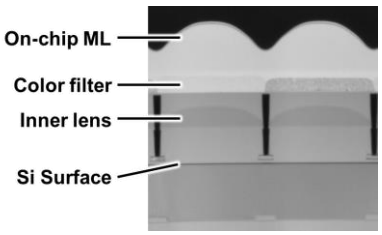

Fig. 4. Cross-sectional image of pixels.

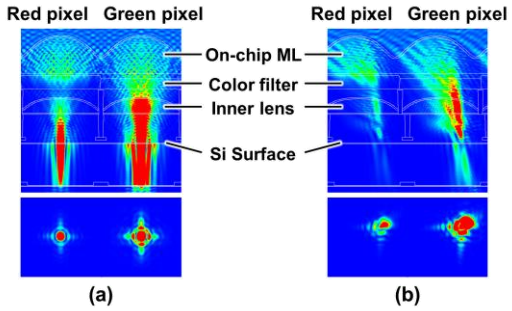

Fig. 5. Optical simulation results for (a) Pixels at the center of chip and (b) Pixels at the edge of chip.

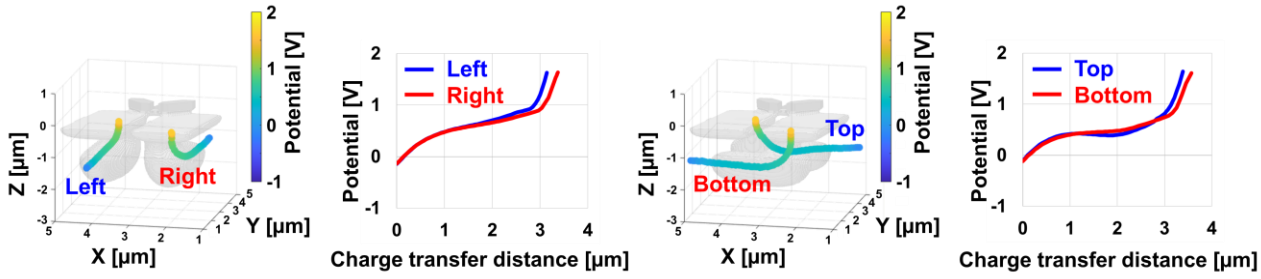

Fig. 6. Potential of charge transfer paths.

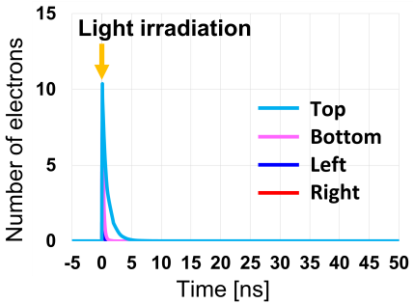

Fig. 7. Number of electrons in the backside photoelectric conversion area.

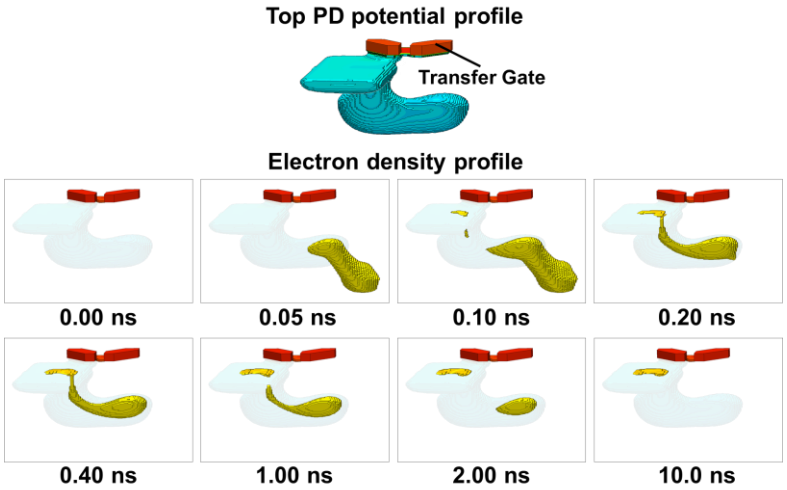

Fig. 8. Current density of top PD at each time after charge generation.

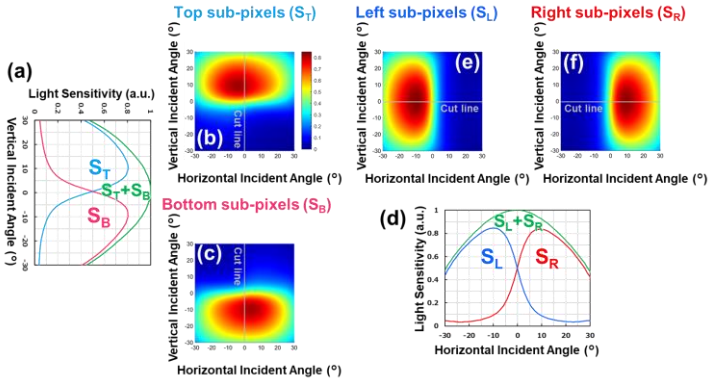

Fig. 9. Light sensitivity dependence on incident angles. (a), (b), (c) Dependence of vertical pixels. (d), (e), (f) Dependence of horizontal pixels.
Signal levels at top, bottom, left, and right sub-pixels are indicated as S_T, S_B, S_L, and S_R, respectively.

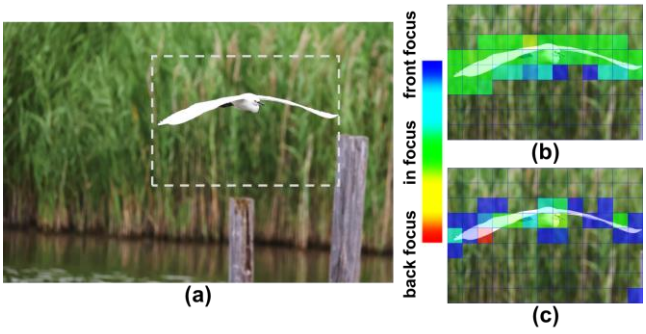

Fig. 10. (a) Captured image of a flying bird taken by CMOS image sensor equipped with twisted PD and the phase detection results taken by (b) Vertical AF and (c) Horizontal AF.

Table 2. Comparison of sensor characteristics.

	This work	H. Kim et al. (ISSCC '23)	T. Jung et al. (ISSCC '22)	Y. Sawai et al. (IISW '21)	E.S. Shim et al. (VLSI '21)	T. Okawa et al. (IEDM '19)	M. Kobayashi et al. (IISW '15)
Pixel size	**6.0μm**	1.28μm	1.0μm	5.6μm	1.4μm	1.6μm	6.4μm
AF direction	**Horizontal / Vertical**	Horizontal / Vertical	Horizontal / Vertical	Horizontal	Horizontal / Vertical	Horizontal	Horizontal
Full well capacity	**121,000 e-**	20,000 e-	10,000 e-	100,000 e-	10,000 e-	—	40,000 e-
Sub-pixel saturation	**41,000 e-**	—	—	—	—	—	—
Sensitivity †	**82,000 e-/lux/s**	6,480 e-/lux/s	3,430 e-/lux/s	—	7,000 e-/lux/s	—	78,000 e-/lx/s
Conversion gain	**125/30.2/15.1 μV/e-**	—	—	152/24.5/11.5 μV/e-	—	—	70 μV/e-
Random noise	**2.2/8.3/16.7 e-rms**	0.98 e-rms	2.0 e-rms	5 / - / 30 e-rms	2.0 e-rms	—	2.5 e-rms
Dynamic range †††	**95dB**	86dB ††	74dB ††	85dB	74dB ††	—	84dB ††
Image lag	**< 1.0 e-**	< 1.0 e-	< 1.0 e-	< 1.0 e-	< 1.0 e-	—	—
AF density	**100 %**	—	—	—	—	100 %	100 %
Minimum AF level	**0.007 lux**	—	—	—	—	1 lux	—

†Measured based on different color temperature light source
††Calculated based on disclosed information
†††Calculated with random noise and FWC